OPEN ACCESS

Bioscience Reports

Crystallographic structure of the turbine *C*-ring from spinach chloroplast F-ATP synthase

Asha Manikkoth BALAKRISHNA*, Holger SEELERT†[1], Sven-Hendric MARX†, Norbert A. DENCHER† and Gerhard GRÜBER*[2]

*Nanyang Technological University, School of Biological Sciences, 60 Nanyang Drive, Singapore 637551, Republic of Singapore
†Physikalische Biochemie, Fachbereich Chemie, Technische Universität Darmstadt, Alarich-Weiss-Str.4, D-64287 Darmstadt, Germany

Synopsis

In eukaryotic and prokaryotic cells, F-ATP synthases provide energy through the synthesis of ATP. The chloroplast F-ATP synthase (CF_1F_O-ATP synthase) of plants is integrated into the thylakoid membrane via its F_O-domain subunits *a*, *b*, *b'* and *c*. Subunit *c* with a stoichiometry of 14 and subunit *a* form the gate for H^+-pumping, enabling the coupling of electrochemical energy with ATP synthesis in the F_1 sector.

Here we report the crystallization and structure determination of the *c*14-ring of subunit *c* of the CF_1F_O-ATP synthase from spinach chloroplasts. The crystals belonged to space group C2, with unit-cell parameters $a = 144.420$, $b = 99.295$, $c = 123.51$ Å, and $\beta = 104.34°$ and diffracted to 4.5 Å resolution. Each *c*-ring contains 14 monomers in the asymmetric unit. The length of the *c*-ring is 60.32 Å, with an outer ring diameter 52.30 Å and an inner ring width of 40 Å.

Key words: CF_1F_O-ATP synthase, *c*-rotor, crystallization, F-ATP synthase, spinach chloroplast.

www.bioscirep.org

Bioscience Reports

INTRODUCTION

The F_1F_O-ATP synthase is a membrane-bound multisubunit complex consisting of two rotary motors in the F_O and F_1 sectors, respectively. The membrane-bound proton translocating ATP synthase of chloroplasts, CF_1F_O catalyses ATP synthesis and ATP hydrolysis coupled to proton translocation across the F_O sector. The chloroplast F_1 domain consists of the subunits $\alpha_3\beta_3\gamma\delta\varepsilon$ [1] and the membrane-integrated CF_O, is made up of the subunits *a*, *b*, *b'* and *c*-ring rotor subunits, which are often named subunit IV, I, II and III, respectively [2,3]. The subcomplex $\alpha_3\beta_3$ forms a hexamer with a central cavity that allows for the penetration of the γ rotor shaft [4]. Subunits γ and ε form the soluble part of the rotor shaft, called the central stalk [5]. Rotation of the central stalk subunit γ within the $\alpha_3\beta_3$ cavity causes conformational changes in the three catalytic sites located at the $\alpha–\beta$ interfaces leading to ATP synthesis [6]. The two parts of ATP synthases are connected by two stalks, i.e. one central rotating shaft formed by the subunits γ and ε and a thin stalk at the periphery, composed of the subunits *b*, *b'* and δ holding together the F_1- and F_O portions [5].

Subunits *a* and *c* are involved in the process of proton-pumping, thereby coupling the events of ATP synthesis and -hydrolysis in the $\alpha_3\beta_3$-hexamer of F_1. A total of ten copies of subunit *c* in yeast F-ATP synthase are found to associate into a ring structure that interacts with the foot of the central stalk subunits in the intact enzyme [7]. The copy number of *c* subunits in the ring has been experimentally studied in different organisms and is found to vary from 8 to 15 among bacterial, yeast, plant and mammalian ATP synthases [2,7–14].

The number of subunits and therefore the diameter of the proton turbine seem to be species dependent [7,8]. Atomic Force Microscopy studies, done by Seelert et al. [2] showed that the protein turbine in F_O of chloroplast ATP synthase has an asymmetric cylindrical structure with 14 symmetrically distributed subunits, which protrude from both membrane surfaces. Here a new protocol has been developed to obtain crystals of the *c*-ring of the spinach chloroplast F-ATP synthase, starting from the intact and active enzyme, which diffracted X-rays to 4.5 Å resolution.

The crystallographic structure shows that each of the fourteen c subunits folds into a hairpin of two TM (transmembrane) helices, connected by a short partially structured loop. The presented $c14$-ring structure is discussed from the perspective of bioenergetic costs in plants.

EXPERIMENTAL

Isolation of enzymatically active chloroplast F-ATP synthase

Chloroplast ATP synthase was isolated from spinach (*Spinacea oleracea* L.) following the procedure described by Pick and Racker [15] with slight modifications as described in [16]. Thylakoid membranes were solubilized using the detergents sodium cholate (23 mM) and octyl-β-D-glucopyranoside (40 mM). For removal of contaminating proteins and lipids, the ATP synthase was subjected to fractionated ammonium sulfate precipitation and sucrose density gradient centrifugation (containing 1 mg/ml asolectin and 8 mM DDM (*n*-dodecyl-β-D-maltoside), to stabilize the protein). Thereafter, the enzyme was purified by dye-ligand chromatography with reactive red 120 [16].

Electrophoresis

BN (blue-native)-PAGE was performed using a Hoefer Mighty Small II SE 250 system (small gel: 10 cm×8 cm×0.15 cm) as described [17,18]. The stacking gel had an acrylamide concentration of 3% and the separating gel an acrylamide gradient from 3.5 to 16%. Approximately 30 μg of solubilized purified CF_1F_O-ATP synthase in DDM was loaded per lane. A high molecular weight native marker (GE Healthcare) served as mass standard.

After electrophoresis the gel was scanned to document the bands stained by BN-PAGE. Subsequently, ATPase activity of the CF_1F_O-ATP synthase was determined by incubating the gel in buffer A1 containing 35 mM Tris, 270 mM glycine, 14 mM $MgSO_4$, 0.2% (w/v) $Pb(NO_3)_2$, 8 mM ATP, pH 7.8 at 37°C for several hours [19,20]. The white lead phosphate precipitate was documented with a CCD-Imaging System (LAS 3000 intelligent dark box, Fujifilm).

SDS–PAGE was performed according to Laemmli [21], with a stacking gel of 3% and separating gel of 14%. In order to maintain integrity of the subunit c oligomer, protein samples were incubated at room temperature (25°C) in SDS loading buffer for 10 min. For visualization of protein bands, the gel was stained with Coomassie R-250.

Measurement of ATP synthesis

To measure the ATP synthesis activity driven by an electrochemical proton gradient, reconstitution of solubilized ATP synthase into liposomes (phosphatidyl choline/phosphatidic acid, 9:1, w/w) was performed as previously described [20]. As a reference, CF_1F_O-ATP synthase was inhibited by adding DCCD (di-cyclohexylcarbodiimid, 50 μM) before reconstitution into liposomes and incubation for 30 min at room temperature [22].

ATP synthesis activity of the CF_1F_O-ATP synthase was measured according to Fischer et al. [23] and Poetsch et al. [24] with slight modifications. 240 μl buffer L2 (200 mM Tricin, 5 mM sodium dihydrogenphosphate, 2.5 mM $MgCl_2$, 120 mM KCl, 0.2 mM ADP, pH 8.3) was added into a clinicon-cuvette and mixed with 12.5 μl Luciferin–Luciferase-reagent (ATP-Monitoring Kit; Thermo Labsystems). The cuvette was placed into a Luminometer (BioOrbit 1250) and the baseline was recorded.

Approximately 43 μl of proteoliposomes were equilibrated with 217 μl buffer L1 (20 mM sodium succinate, 5 mM sodium dihydrogenphosphate, 2.5 mM $MgCl_2$, 0.6 mM KCl, 1 μM Valinomycin, pH 4.7). After 100 s, the mixture was injected via a cannula into the cuvette containing L2. ATP synthesis, driven by the established TM electrochemical gradient (ΔpH and ΔK^+), was monitored as luminescence applying the Luciferin–Luciferase-Assay. For calibrating the luminescence signal, 20 μl of 10 μM ATP was added.

Crystallization trials of CF_1F_O-ATP synthase from spinach chloroplast

Initial screens of the entire CF_1F_O-ATP synthase at a concentration of 18 mg/ml were set up using the Memplus screen from Molecular Dimensions, UK, using the vapour diffusion method. In several drops, phase separation was observed and systematic variations of pH, precipitant and protein concentration were done to promote nucleation. Crystals grew out of the phase and took approximately 2 months to appear under optimized conditions and cryo freezed in 50% (v/v) mineral oil and paratone. Crystals were analysed at the Swiss Light Source and diffracted to 4.5 Å.

Data collection

A single wavelength dataset of the CF_1F_O crystal was collected at the protein crystallography beamline S06 PX at the SLS (Swiss Light Source) with a PILATUS 6M detector. Data were collected as a series of 0.2° oscillation images with 10 s exposure time and a detector distance of 500 mm. All diffraction data were indexed, integrated using the iMosflm program [25] and reduced with SCALA [26] and CTRUNCATE [27]. The results of data processing and data statistics are summarized in Table 1.

Structure solution and refinement

The structure of the c-rotor of CF_1F_O-ATP synthase was determined by molecular replacement using the coordinates of the c-rotor of the proton-translocating chloroplast ATP synthase [12] [PDB (Protein Data Bank) code 2W5J]. Only the main chain atoms of the model were used for structure solution. Molecular replacement was performed using the PHASER program (TFZ = 11.7, LLG score = 963, [28]). Since anisotropy was observed in the data, they were subjected to ellipsoidal truncation and anisotropic scaling using the program SCALEIT, which is

Statistics of crystallographic data collection	
Wavelength (Å)	1.00
Space group	C2
Unit cell	$a = 144.420$, $b = 99.295$, $c = 123.51$Å
	$\beta = 104.34°$
Resolution range (Å)	30 – 6.0 (6.32-6.0)
No. of unique reflections	4238
Total no. of reflections	12041
Multiplicity	2.8 (2.8)
Completeness (%)	97.6 (98.37)
I/sigma	9.6 (5.3)
R_{merge} *	0.049 (0.106)
Mosaicity	0.82

*$R_{merge} = \Sigma\Sigma_i|I_h - I_{hi}|/\Sigma\Sigma_i\ I_h$, where I_h is the mean intensity for reflection h.

integrated in CCP4 (Collaborative Computational Project No. 4) [29]. Diffraction anisotropy was evidenced as a directional dependence in diffraction quality. The crystal diffracted to 4.5 Å in the horizontal direction and to 6.0 Å in the vertical direction. This kind of anisotropy is attributed to whole-body anisotropic vibration of unit cells, resulting in the crystal packing interactions being more uniform in one direction than in the other. Therefore, the R-factors were stalled at one stage during refinement and hence the data resolution was truncated at 6.0 Å. The model was manually corrected in COOT [30] and refined in REFMAC [31]. Many cycles of model building and restrained refinement with tight geometric restraints were carried using overall temperature factor and NCS (non-crystallographic symmetry) restraints. Density modification was carried out by DM in the CCP4 suite. ProSMART (Procrustes Structural Matching Alignment and Restraint Tool) was used for generation of external restraints for the refinement [32]. The PDB ID 2W5J was used as reference for exercising this restraint. In the final REFMAC cycles, TLS (translation, libration, screw) procedure was applied. The structure was validated using PROCHECK [33]. All the figures were drawn using PYMOL [34]. Structural comparison analysis are carried out using the SUPERPOSE program [35]. The atomic coordinates and structure factors have been deposited in the PDB (ID: 4MJN).

RESULTS AND DISCUSSION

Biochemical characterization of the entire CF_1F_O-ATP synthase

The complete chloroplast F_1F_O-ATP synthase from spinach, used for crystallization, was characterized by different methods. The enzyme showed high purity as revealed by SDS–PAGE (Figure 1A) and BN-PAGE (1B). In the SDS gel, the bands of all subunits were present and subunit c (III) migrated as an intact oligomer (Figure 1B). Besides purity, the BN gel demonstrated the presence of predominantly intact CF_1F_O-ATP synthase (mass of >500 kDa in Figure 1B). Only a small proportion of unbound CF_1 is present, but no CF_O. These indicate that the crystallized c14-cylinder emerged from the intact enzyme. Additionally, the in-gel assay of ATP hydrolysis demonstrates the preservation of the enzymatic activity of the isolated ATP synthase preparation (results not shown). Since ATP hydrolysis in intact chloroplast ATP synthases is strictly regulated by the subunits ε and γ and other effectors [20], this activity assay can only provide a first indication of functional integrity. Therefore ATP synthesis activity of the CF_1F_O-ATP synthase was examined (Figure 1C). This was achieved by reconstitution of the entire CF_1F_O-ATP synthase into liposomes and application of an electrochemical proton gradient. With this method, an ATP synthesis activity of 41 ± 4 ATP per enzyme per second was determined.

Crystallization and preliminary X-ray analysis

The enzymatically active and entire CF_1F_O-ATP synthase was used for crystallization and crystals of good diffraction quality appeared from the optimized phase separated drop under conditions of 33 % (v/v) PEG 550 MME, 0.05 M sodium acetate pH 4.3 (Figure 1D). The crystals were colourless, in contrast to recently obtained yellow crystals, which were described to contain one chlorophyll and two carotenoids [3]. However, no protein structure from this crystal form has yet been described [3].

The crystals obtained diffracted to 4.5 Å resolution and belonged to C2 space group ($\beta = 104.34°$), with unit-cell parameters $a = 144.42$, $b = 99.29$, and $c = 123.51$ Å. The phases were obtained using the crystal structure of the c14 rotor ring of the chloroplast F-ATP synthase (PDB ID 2W5J [12]. The solvent content was calculated to be 63.45 % and V_m was 3.36 Å^3 per Da [36].

Analysis of the data as well as the solution from molecular replacement confirmed that only the c-ring rotor of the chloroplast ATP synthase is present in the crystal structure, whereas all the F_1 subunits α, β, γ, δ and ε and subunits a, b and b' of the membrane-integral F_O domain are lost during the crystallization process. The initial electron density map also suggests that most probably only the c-ring is present in the crystal structure.

Overall structure of the c-rotor

The structure of the c-rotor of the spinach chloroplast F-ATP synthase was determined by the molecular replacement method and refined to 6.0 Å. A summary of the refinement statistics is given in Table 2. Analysis of the stereochemical quality of the final model by PROCHECK has identified that 97 % of all the residues are within the core regions of the Ramachandran plot, 2.1 % are within the allowed regions, and 0.9 % are within the generously allowed region. No residues are present in the disallowed region. The last four C-terminal amino acids are not visible in the electron
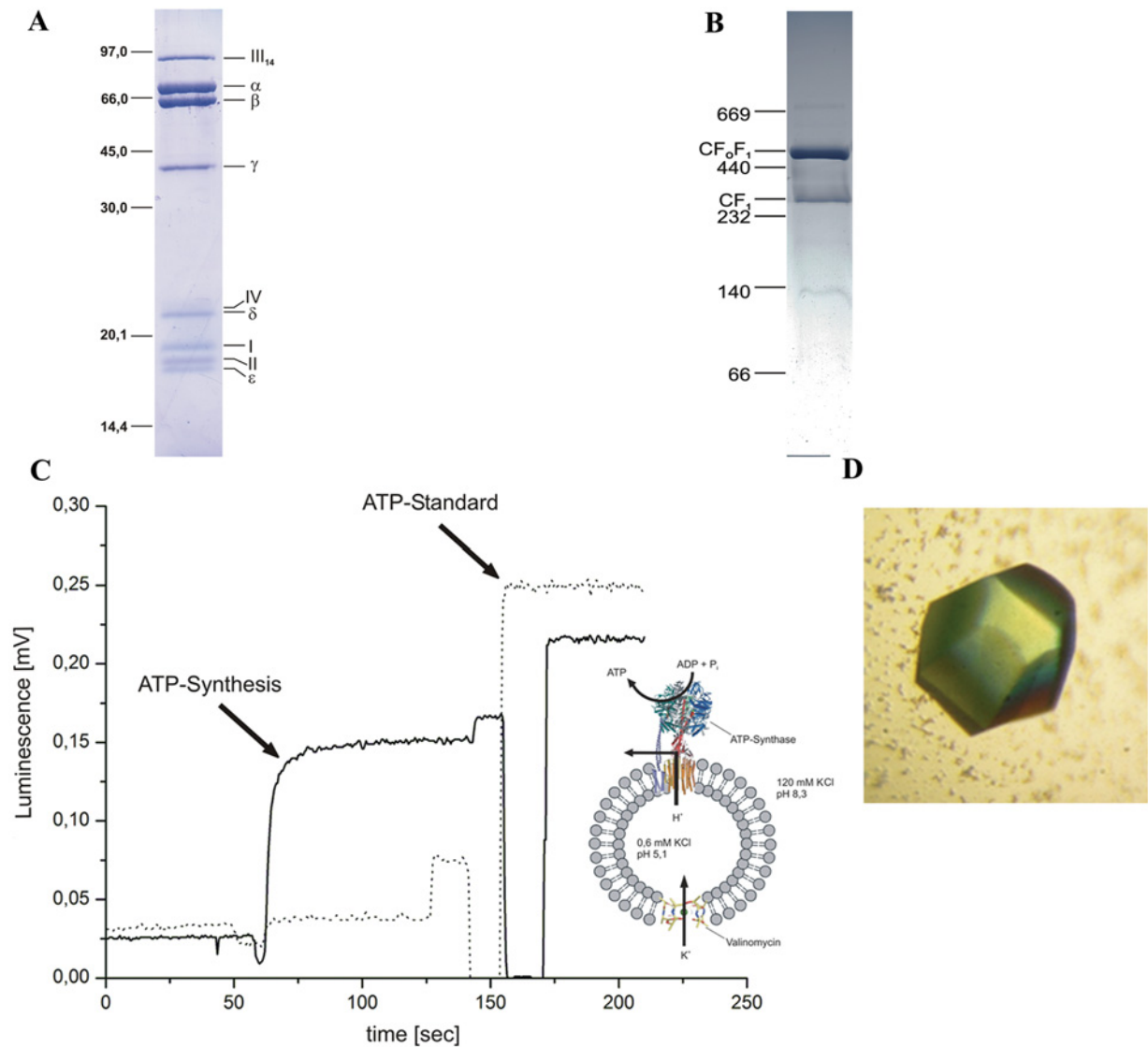
Figure 1   Biochemical and functional characterization of the purified chloroplast F-ATP synthase
(**A**) SDS gel (14% total acrylamide and 4% cross-linked acrylamide) of the purified CF_1F_O-ATP synthase from spinach chloroplasts. The gel reveals the F_1 subunits $\alpha_3\beta_3\gamma\delta\varepsilon$ and the CF_O subunits b, b', c and a, respectively, which are also called I, II, III and IV in plants. Subunit c (III) migrates as a 14-protomer entity. (**B**) BN gel Coomassie Brilliant Blue stained of 30 μg CF_1F_O-ATP synthase isolated from spinach chloroplasts. (**C**) ATP synthesis activity of CF_1F_O-ATP synthase of *Spinacea oleracea*. The graph demonstrates the generation of ATP, induced by an electrochemical H^+/K^+ gradient. To demonstrate that ATP is only produced by the ATP-synthase, the measurements were also performed with CF_1F_O-ATP synthase inhibited by DCCD treatment before reconstition (dotted line). (**D**) Crystal of the c-ring from spinach chloroplast CF_1F_O-ATP synthase.

density map. Validation with ERRAT server gave an overall quality factor of 97.03% [37]. The rmsd (root-mean-square distance) between the presented structure and the previously determined c-ring of the chloroplast ATP synthase (2W5J [12]) is 1.509 Å. The overall structure of the spinach chloroplast c-ring is shown in Figures 2(A) and 2(B). Each subunit c folds into a hairpin of two TM helices, connected by a short partially structured loop (Figure 2E). The individual hairpin, composed of an N-terminal TM and a C-terminal TM, produce an inner- and an outer ring.

The N-terminal helices face the inner side of the ring, whereas the C-terminal helices face the outside of the loop. This arrangement facilitates interaction of the conserved glutamic acid residues of subunit c (Figure 3) with the conserved Arginine residue from subunit a, providing the structural requirements to form a part of the proton channel in the F_O domain. Figures 2(C) and 2(D) display the electrostatic charge surface of this rotary entity. The cytoplasmic and the luminal surfaces of the c ring are very polar in nature as they are in contact with the aqueous phase. The
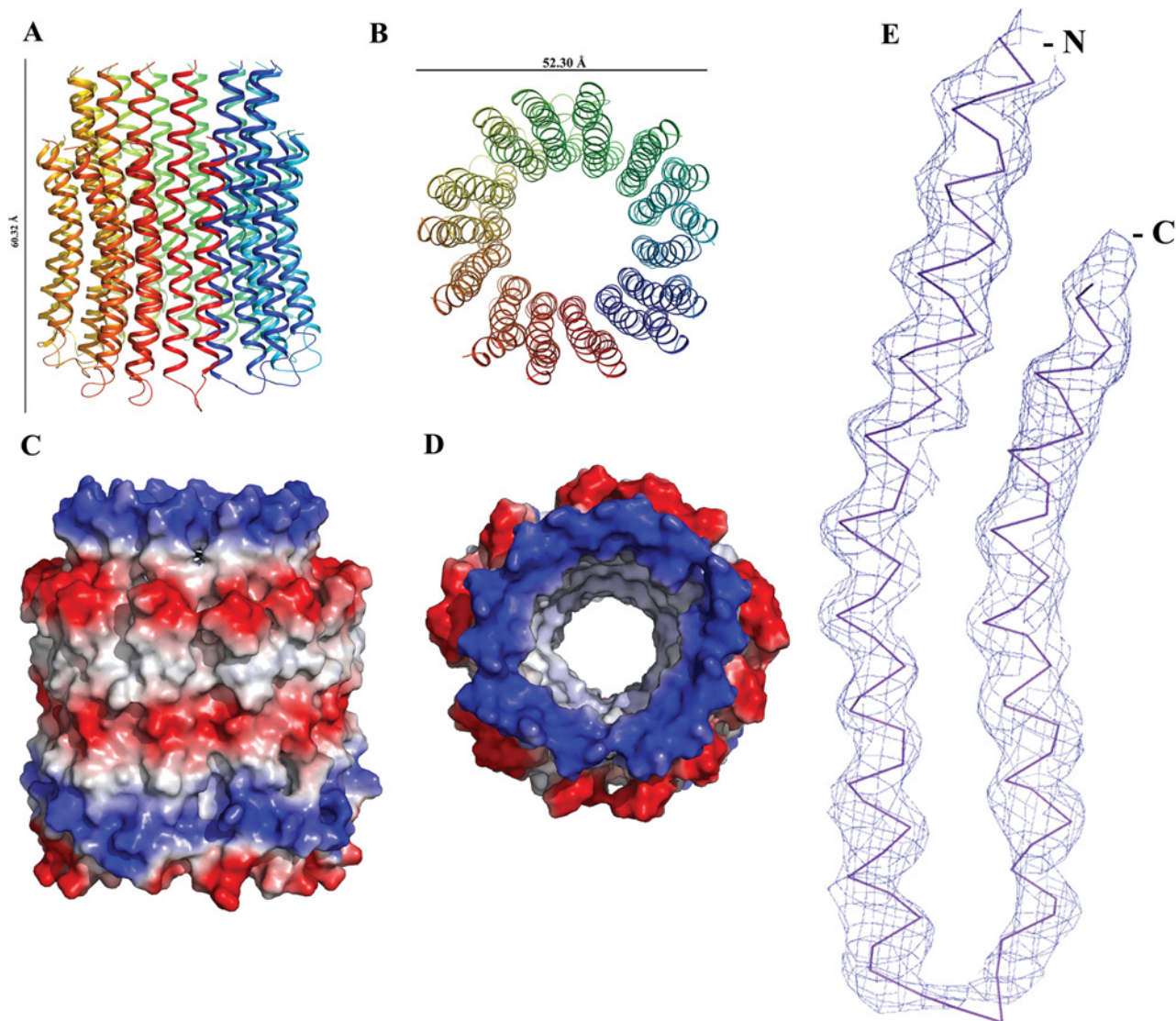
Figure 2   The structure of the *c*-ring of the spinach chloroplast F-ATP synthase
(**A**) Cartoon representation of the *c*-ring in side view and (**B**) view from the lumen. (**C**) The electrostatic potential (calculated in pymol [34]) mapped on the surface of the *c*-ring with positive areas in blue, negative in red, and neutral in white colour, in side view. (**D**) The electrostatic potential mapped on the surface of the *c*-ring, the view is from the lumen. (**E**) Electron density map ($2F_o$-F_c) of chain A at 1σ for the *c*-ring.

hydrophilic patch at the centre of the membrane region represents the proton-binding site.

The length of the spinach chloroplast *c*-ring assembly is 60.32 Å long. The outer ring diameter is 52.3 Å, and the inner ring has a width of 40 Å. The inner space would be wide enough to accommodate detergent molecules. Interestingly, electron density could be observed in the initial maps in this region. However, this cannot be confirmed at this moderate resolution. Previously studies of 2D crystals of the intact CF_O or $c_{14}a$ complex by AFM and Cryo-electron microscopy revealed distinct mass/electron density inside and protruding from the *c*14-cylinder. The isolated

*c*14-cylinder, however, was 'empty' [41,42]. The electron density for the hairpin was continuous. Because of the achieved resolution, only the density for the main chains could be identified (Figure 2E).

The crystal lattice reveals one *c*-ring consisting of 14 monomers (*c*14 ring) in the asymmetric unit forming crystal contacts with three neighbouring rings. The $\kappa = 180°$ section of the self-rotation function, calculated for the crystal form using MOLREP (Collaborative Computational Project No. 4) with an integration radius of 20.0 Å and data in the resolution range 15–6 Å, showed a string of 14 peaks. The loop region of one ring
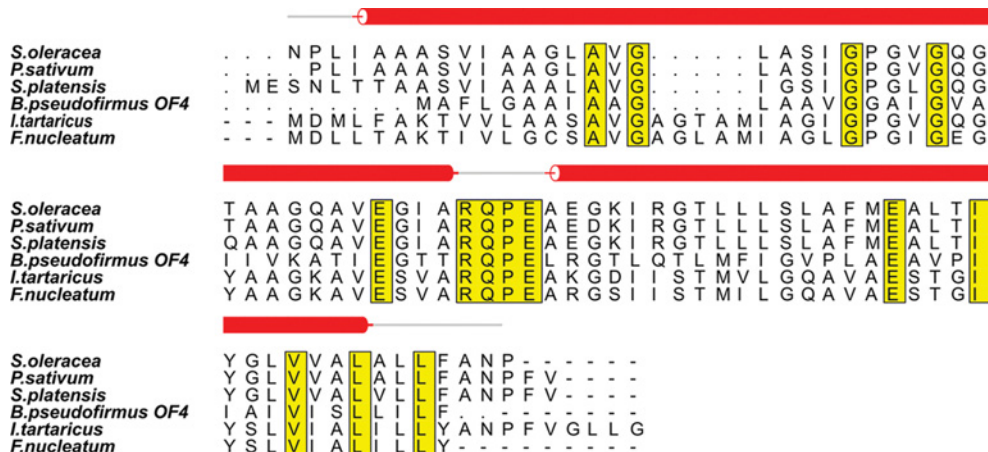
Figure 3   Multiple sequence alignment of c subunits of F-ATP synthases from *Spinacia oleracea, Pisum sativum, Spirulina platensis, Bacillus pseudofirmus OF4, Ilyobacter tartaricus* and *Fusobacterium nucleatum*

All the conserved residues are highlighted in yellow. The sequence of Spinach chloroplast c subunit along with its secondary structure was aligned to related homologous structures. The secondary structures are drawn in red. The figure was generated using ALSCRIPT.

Table 2 Refinement statistics

Refinement statistics	
*R factor(%)	35.3
†R free(%)	37.8
Ramachandran statistics	
Most favored (%)	97
Additionally allowed (%)	2.1
Generously (%)	0.9
Disallowed (%)	0.0
R.M.S. deviations	
Bond lengths (Å)	0.019
Bond angles (°)	2.019
Mean atomic B values (Å^2)	
Overall	39.72

*R-factor = $\Sigma\|F_O| - |F_C\|/\Sigma|F_O|$, where F_O and F_C are measured and calculated structure factors, respectively.
†R-free = $\Sigma\|F_O| - |F_C\|/\Sigma|F_O|$, calculated from 5% of the reflections selected randomly and omitted from the refinement process.

is in close contact with the loop region of its symmetry mate. The other two points of contact in the crystal lattice involves the monomers in the N-terminal region.

Comparison with *c*-rotors of other organisms

Crystallographic structures of the *c*-ring rotors have been reported for F-ATP synthases from *Ilyobacter tartaricus* [9], *Spirulina platensis* [13], *Pisum sativum* [38] and *Saccharomyces cerevesiae* [7,10]. Among all the *c*-ring structures, only the spinach and pea chloroplasts are related by tetradecameric symmetry in the asymmetric unit. Despite this similarity, the two display markedly different shapes, with the *c*-ring of *P. sativum* taking up a concave

barrel shape with a pronounced waist in the middle, whereas that of spinach chloroplast has a much less pronounced concave curvature.

The diameters of these *c*-ring rotors differ from organism to organism, because of the variation in the number of protomers. The undecameric *c*-ring of *I. tartaricus* shows a cylindrical, hourglass shaped protein complex with an outer diameter of ∼50 Å and inner diameter of ∼17 Å [9]. The pea chloroplast *c*-ring has an outer ring diameter of 60.5 Å and an inner ring diameter of 35 Å [38]. The *c*15 ring from *S. platensi*s has an hour glass shaped assembly with an outer diameter of 65 Å and an inner diameter of 54 Å [13]. The yeast *c*-ring diameter in the F_1c10 complex structure is ∼55 Å and the inner diameter is ∼27 Å and comprises ten protomers [7]. In comparison, the spinach chloroplast *c*14 ring presented here has an external diameter of 52.30 Å, whereas that of the inner ring is 40 Å. From the perspective of bioenergetic costs 14 protons have to be translocated across the thylakoid membrane per full rotation of the rotary *c*-ring, whereby each rotation of 360° produces three molecules of ATP in the $\alpha_3\beta_3$-headpiece of F_1. Therefore 3.7 protons are needed to synthesize one molecule of ATP in the spinach chloroplast F-ATP synthase. In comparison, 2.7 protons per ATP are required for the bovine mitochondrial F-ATP synthase, whose *c*-ring consists of eight *c* subunits [8], reflecting a more efficient enzyme with respect to protons consumed per ATP generated, at least at first glance. However, the two components of the proton-motive force, i.e. the membrane potential and the pH gradient, are kinetically not equivalent and different sizes of the cation-powered rotors may be nature's solution to cope with the challenges of diverse environments [42].

Recently, two more *c*-ring crystal structures have been solved, one from *Fusobacterium nucleatum*, which has 11 protomers [39], and the other from *Bacillus pseudofirmus OF4*, which has 13 protomers [40]. These studies demonstrated that the alanine

motif in the $c13$-ring from *B. pseudofirmus OF4* contributes to high complex stability, with A-to-G mutations reducing the c-ring stoichiometry, in this case from $c13$ to $c12$, whereas G-to-A mutations increases it. From the sequence alignment in Figure 3, it can be seen that the $c11$-ring of *I. tartaricus* consists of 17.8 % alanine residues compared with an alanine content of 21.8 % in the $c14$-ring of the spinach chloroplast F-ATP synthase investigated here.

There is urgent need to determine the structure of the intact CF_O turbine, in order to elucidate the spatial arrangement of the subunits b and b', and especially of subunit a in relation to the $c14$-ring. This would also lead to an answer to the pertinent question of how the c-ring is made proton-tight so as to prevent harmful proton leaks across its central structure, that would otherwise bypass the specific proton pathway between subunit a and the c subunits.

AUTHOR CONTRIBUTION

ACKNOWLEDGEMENTS

FUNDING

REFERENCES

1   Boekema, E. J., van Heel, M. and Gräber, P. (1998) Structure of chloroplast F_1 ATPase studied by electron microscopy and image processing. Biochim. Biophys. Acta **933**, 365–371

2   Seelert, H., Poetsch, A., Dencher, N. A, Engel, A., Stahlberg, H. and Müller, D. J. (2000) Structural biology. Proton-powered turbine of a plant motor. Nature **405**, 418–419

3   Varco-Merth, B., Fromme, R., Wang, M. and Fromme, P. (2008) Crystallization of the c14-rotor of the chloroplast ATP synthase reveals that it contains pigments. Biochim. Biophys. Acta **1777**, 605–612

4   Abrahams, J. P, Leslie, A. G. W., Lutter, R. and Walker, J. E (1994) Structure at 2.8-angstom resolution of F1-ATPase from bovine heart-mitochondria. Nature **370**, 621–628

5   Junge, W., Lill, H. and Engelbrecht, S. (1997) ATP synthase: an electrochemical transducer with rotatory mechanics. TIBS **22**, 420–423

6   Gibbons, C., Montgomery, M. G., Leslie, A. G. W. and Walker, J. E (2000) The structure of the central stalk in bovine F(1)-ATPase at 2.4 A resolution. Nat. Struct. Biol. **7**, 1055–1061

7   Stock, D., Leslie, A. G. W. and Walker, J. E. (1999) Molecular architecture of the rotary motor in ATP synthase. Science **286**, 1700–1705

8   Watt, I. N., Montgomery, M. G., Runswick, M. J., Leslie, A. G. W. and Walker, J. E. (2010) Bioenergetic cost of making an adenosine triphosphate molecule in animal mitochondria. Proc. Natl. Acad. Sci. U.S.A. **107**, 16823–16827

9   Meier, T., Polzer, P., Diederichs, K., Welte, W. and Dimroth, P. (2005) Structure of the rotor ring of F-Type Na^+-ATPase from *Ilyobacter tartaricus*. Science **308**, 659–662

10 Symersky, J., Pagadala, V., Osowsk, D., Krah, K., Meier, T., Faraldo-Gómez, J. D. and Mueller, D. M. (2012) Structure of the c(10) ring of the yeast mitochondrial ATP synthase in the open conformation. Nat. . Struct. Mol. Biol. **19**, 485–491

11 Matthies, D., Preiss, L., Klyszejko, A. L., Müller, D. J., Cook, G. M., Vonck, J. and Meier, T. (2009) The c13 ring from a thermoalkaliphilic ATP synthase reveals an extended diameter due to a special structural region. J. Mol. Biol. **388**, 611–618

12 Vollmar, M., Schlieper, D., Winn, M., Buchner, C. and Groth, G. (2009) Structure of the c14 rotor ring of the proton translocating chloroplast ATP synthase. J. Biol. Chem. **284**, 18228–18235

13 Murshudov, G. N., Vagin, A. A. and Dodson, E. J. (1997) Refinement of macromolecular structures by the maximum-likelihood method. Acta Crystallogr. D **53**, 240–255

14 Pogoryelov, D., Krah, A., Langer, J. D., Yildiz, O., Faraldo-Gómez, J. D. and Meier, T. (2010) Microscopic rotary mechanism of ion translocation in the F(o) complex of ATP synthases. Nat. Chem. Biol. **6**, 891–899

15 Pick, U. and Racker, E. (1979) Purification and reconstitution of the N,N′-dicyclohexylcarbodiimide-sensitive ATPase complex from spinach chloroplasts. J. Biol. Chem. **254**, 2793–2799

16 Seelert, H., Poetsch, A., Rohlfs, M. and Dencher, N. A. (2000) Dye-ligand chromatographic purification of intact multisubunit membrane protein complexes: application to the chloroplast H^+-$F_O F_1$-ATP synthase. Biochem. J. **346**, 41–44

17 Neff, D. and Dencher, N. A. (1999) Purification of multisubunit membrane protein complexes: isolation of chloroplast $F_O F_1$–ATP synthase, CF_O and CF_1 by blue native electrophoresis. Biochem. Biophys. Res. Commun. **259**, 569–575

18 Krause, F. and Seelert, H. (2008) Detection and analysis of protein-protein interactions of organellar and prokaryotic proteomes by blue native and colorless native gel electrophoresis. Curr. Protoc. Protein Sci. **51**, 14.11.1–14.11.36

19 Zerbetto, E., Vergani, L. and Dabbeni-Sala, F. (2000) Quantification of muscle mitochondrial oxidative phosphorylation enzymes via histochemical staining of blue native polyacrylamide gels. Electrophoresis **18**, 2059–2064

20 Suhai, T., Heidrich, N. G., Dencher, N. A. and Seelert, H. (2009) Highly sensitive detection of ATPase activity in native gels. Electrophoresis **30**, 3622–3625

21 Laemmli, U. K. (1970) Cleavage of structural proteins during the assembly of the head of bacteriophage T_4. Nature **227**, 680–685

22 Suhai, T., Dencher, N. A., Poetsch, A. and Seelert, H. (2008) Remarkable stability of the proton translocating $F_1 F_O$-ATP synthase from the thermophilic cyanobacterium *Thermosynechococcus elongatus* BP-1. Biochim. Biophys. Acta **1778**, 1131–1140

23 Fischer, S., Etzold, C., Turina, P., Deckers-Hebestreit, G., Altendorf, K. and Gräber, P. (1994) ATP synthesis catalyzed by the ATP synthase of *Escherichia coli* reconstituted into liposomes. Eur. J. Biochem. **225**, 167–172

24 Poetsch, A., Rexroth, S., Heberle, J., Link, T., Dencher, N. A. and Seelert, H. (2003) Characterisation of subunit III and its oligomer from spinach chloroplast ATP synthase. Biochim. Biophys. Acta **1618**, 59–66

25 Battye, T. G. G., Kontogiannis, L., Johnson, O., Powell, H. R. and Leslie, A. G. W. (2011) iMOSFLM: a new graphical interface for diffraction-image processing with MOSFLM. Acta Crystallogr. D **67**, 271–281

26 Evans, P. (2006) Scaling and assessment of data quality. Acta Crystallogr. D **62**, 72–82

27 French, G. and Wilson, K. (1978) On the treatment of negative intensity observations. Acta Crystallogr. A **34**, 517–525

28 McCoy, A. J., Grosse-Kunstleve, R. W., Adams, P. D., Winn, M. D., Storoni, L. C. and Read, R. J. (2007) Phaser crystallographic software. J. Appl. Crystallogr. **40**, 658–674

29 Dyda, F. (2010) Developments in low-resolution biological X-ray crystallography. Biol. Rep. **2**, 80–82

30 Emsley, P. and Cowtan, K. (2004) COOT: model-building tools for molecular graphics. Acta Crystallogr. D **60**, 2126–2132

31 Murshudov, G. N., Vagin, A. A. and Dodson, E. J. (1997) Refinement of macromolecular structures by the maximum-likelihood method. Acta Crystallogr. D **53**, 240–255

32 Nicholls, R. A., Long, F. and Murshudov, G. N. (2012) Low-resolution refinement tools in REFMAC5. Acta Crystallogr. D **68**, 404–417

33 Laskowski, R. A., MacArthur, M. W., Moss, D. S. and Thorton, J. M. (1993) PROCHECK: a program to check the stereochemical quality of protein structures. J. Appl. Crystallogr. **26**, 283–291

34 DeLano, W. L. (2002) The Pymol molecular graphics system. DeLano Scientific, USA

35 Krissinel, E. and Henrick, K. (2004) Secondary-structure matching (SSM), a new tool for fast protein structure alignment in three dimensions. Acta Crystallogr. D **60**, 2256–2268

36 Matthews, B. W. (1968) Solvent content of protein crystals. J. Mol. Biol. **33**, 491–497

37 Colovos, C. and Yeates, T. O. (1993) Verification of protein structures: patterns of nonbonded atomic interactions. Protein Sci. **2**, 1511–1519

38 Saroussi, S., Schushan, M., Ben-Tal, N., Junge, W. and Nelson, N. (2012) Structure and flexibility of the c-ring in the electromotor of rotary F(0)F(1)-ATPase of pea chloroplasts. PloS ONE **7**, e43045

39 Schulz, S., Iglesias-Cans, M., Krah, A., Yildiz, O., Leone, V., Matthies, D., Cook, G. M., Faraldo-Gómez, J. D. and Meier, T. (2013) A new type of Na$^{(+)}$-driven ATP synthase membrane rotor with a two-carboxylate ion-coupling motif. PLoS Biol. **6**, e1001596

40 Preiss, L., Klyszejko, A. L., Hicks, D. B., Liu, J., Fackelmayer, O. J., Yildiz, Ö., Krulwich, T. A. and Meier, T. (2013) The c-ring stoichiometry of ATP synthase is adapted to cell physiological requirements of alkaliphilic Bacillus pseudofirmus OF4. Proc. Natl. Acad. Sci. U.S.A. **110**, 7874–7879

41 Seelert, H., Dencher, N. A. and Müller, D. J. (2003) Fourteen protomers compose the oligomer III of the proton-rotor of spinach chloroplast ATP-synthase. J. Mol. Biol. **333**, 337–344

42 Seelert, H., Dani, D. N., Dante, S., Hauβ, T., Krause, F., Schäfer, E., Frenzel, M., Poetsch, A., Rexroth, S., Schwaβmann, H. J. et al. (2009) From protons to OXPHOS supercomplexes and Alzheimer's disease: structure-dynamics-function relationships of energy-converting membranes. Biochim. Biophys. Acta **1787**, 657–671